

An adaptive kernel-split quadrature method for parameter-dependent layer potentials

Ludvig af Klinteberg^{*1}, Fredrik Fryklund², and Anna-Karin Tornberg²

¹*Department of Mathematics, Simon Fraser University, Burnaby, Canada*

²*Department of Mathematics, KTH Royal Institute of Technology, Stockholm, Sweden*

Abstract

Panel-based, kernel-split quadrature is currently one of the most efficient methods available for accurate evaluation of singular and nearly singular layer potentials in two dimensions. However, it can fail completely for the layer potentials belonging to the modified Helmholtz, biharmonic and Stokes equations. These equations depend on a parameter, denoted α , and kernel-split quadrature loses its accuracy rapidly when this parameter grows beyond a certain threshold. The present report describes an algorithm that remedies this problem, using per-target adaptive sampling of the source geometry. The refinement is carried out through recursive bisection, with a carefully selected rule set. This maintains accuracy for a wide range of α , at an increased cost that scales as $\log \alpha$. Using this algorithm allows kernel-split quadrature to be both accurate and efficient for a much wider range of problems than previously possible.

1 Introduction

This report presents an extension to the panel-based, kernel-split quadrature scheme by Helsing and Ojala [9], for evaluating singular and nearly singular layer potentials in two dimensions. This scheme represents one of the current state of the art methods for maintaining low errors when solving elliptic partial differential equations (PDEs) in two dimensions using integral equation methods [9, 7, 13]. However, there exists a set of problems for which this scheme can fail completely. This includes the following PDEs in \mathbb{R}^2 :

$$(\Delta u - \alpha^2)u = 0, \quad \text{modified Helmholtz,} \quad (1)$$

$$\Delta(\Delta u - \alpha^2)u = 0, \quad \text{modified biharmonic,} \quad (2)$$

$$(\Delta u - \alpha^2)u - \nabla p = 0, \quad \text{modified Stokes (subject to } \nabla \cdot u = 0), \quad (3)$$

where α is real number. For brevity, we refer to them as the *modified* PDEs. Note that they are not consistently named in the literature. For example, the modified Helmholtz equation is also known as the screened Poisson equation, the Yukawa equation, the linearized Poisson-Boltzmann equation, and the Debye-Hückel equation. Meanwhile, the modified Stokes equations are also known as the Brinkman equations. These PDEs appear in many different applications: electrostatic interactions in protein and related biological functions, macroscopic electrostatics

^{*}Corresponding author. E-mail address: jafklint@sfu.ca

and fluid flow on the micro scale, to mention a few [15, 14, 10, 11, 5, 8]. They also appear as a result of applying implicit or semi-implicit time marching schemes to the heat equation and the time-dependent Stokes and Navier-Stokes equations [4, 6].

A common trait of the modified PDEs is that their associated layer potentials have kernels that either decay exponentially, or have components that decay exponentially, with a rate that is proportional to α . This decay presents a problem for the abovementioned kernel-split quadrature. In short, the quadrature method is based on writing the kernel on a form with smooth functions multiplying explicit singularities, and then integrating each term separately. In order to be accurate, these smooth functions have to be well approximated by piecewise polynomials, which is no longer the case when α is large.

We have developed a robust quadrature scheme, based on adaptive refinement, that maintains high accuracy for any α , without sacrificing efficiency. It applies for target points both on and close to the boundary, where regular quadrature is insufficient. In this context, refinement refers simply to an interpolation of known quantities to a locally refined discretization, as opposed to increasing the number of degrees of freedom in the discretized integral equation.

This report presents a work in progress, as the guidelines for setting parameters are entirely heuristic at the moment, even though they provide very satisfying result. We will at a later date update this report with analysis that supports these parameter choices.

The remainder of this report is organized as follows. In section 2 we give an outline of the kernel-split quadrature. Section 3 describes the problem that we are trying to solve, using the modified Helmholtz equation as an example. The new algorithm we propose is presented in section 4, followed by numerical results in section 5.

2 Background

Our goal is to evaluate layer potentials of the form

$$u(x) = \int_{\partial\Omega} G(x, y) \sigma(y) \, dS(y). \quad (4)$$

The layer density $\sigma(y)$ is assumed to be smooth, while the kernel $G(x, y)$ is singular at $x = y$. It can be expressed with explicit singularities as

$$G(x) = G_0(x, y) + G_L(x, y) \log|x - y| + G_C(x, y) \frac{(x - y) \cdot \hat{n}(y)}{|x - y|^2}, \quad (5)$$

where G_0 , G_L and G_C are smooth functions. We refer to this decomposition as kernel-split.

The boundary $\partial\Omega$ is discretized using a composite Gauss-Legendre quadrature. It is subdivided into intervals, denoted *panels*,

$$\partial\Omega = \bigcup_i \Gamma_i. \quad (6)$$

Each panel Γ_i is described by a parametrization γ_i ,

$$\Gamma_i = \{\gamma_i(t) \mid t \in [-1, 1]\}. \quad (7)$$

Associated with the parametrization is a speed function $s_i(t) = |\gamma_i'(t)|$, a normal vector $\hat{n}_i(t)$ and the curvature $\kappa_i(t)$. Introducing the convenience notation $\sigma_i(t) = \sigma(\gamma_i(t))$, the layer potential from a panel Γ_i becomes

$$\int_{\Gamma_i} G(x, y) \sigma(y) \, dS(y) = \int_{-1}^1 G(x, \gamma_i(t)) \sigma_i(t) s_i(t) \, dt. \quad (8)$$

Each panel is discretized in the parametrization variable t using the nodes and weights (t_j^G, λ_j^G) of an n -point Gauss-Legendre quadrature rule, which is of order $2n$, such that on each panel we have the discrete quantities

$$y_{ij} = \gamma_i(t_j^G), \quad \hat{n}_{ij} = \hat{n}_i(t_j^G), \quad \sigma_{ij} = \sigma(\gamma_i(t_j^G)), \quad (9)$$

$$s_{ij} = \left| \gamma'_i(t_j^G) \right|, \quad \kappa_i = \kappa(t_i^G). \quad (10)$$

Omitting the panel index i , the layer potential contribution from a panel Γ is then computed using the approximation

$$\int_{\Gamma} G(x, y) \sigma(y) dS(y) \approx \sum_{j=1}^n G(x, y_j) \sigma_j s_j \lambda_j^G. \quad (11)$$

Due to the singularities in G , the above formula requires x to be well-separated from Γ (this notion will be clarified further). Otherwise, the scheme of [7] is used, known as product integration. With that, target-specific quadrature weights of order n are computed for the known singularities where needed, such that

$$\int_{\Gamma} f(x, y) \log|x - y| dS(y) \approx \sum_{j=1}^n f(x, y_j) w_j^L(x), \quad (12)$$

$$\int_{\Gamma} f(x, y) \frac{(x - y) \cdot \hat{n}(y)}{|x - y|^2} dS(y) \approx \sum_{j=1}^n f(x, y_j) w_j^C(x). \quad (13)$$

Substituting (5) into (4) and applying the above product integration gives the so called *kernel-split quadrature scheme*. By formulating it as a correction, we only need to explicitly evaluate G_0 at $x = y$. Depending on the location of the target point x relative to the source panel Γ , the evaluation can be divided up into three different cases:

1. **Singular, with self-interaction.** If $x \in \Gamma$ is one of the quadrature nodes, $x = y_i$, then the term multiplying G_C is smooth, with the limit

$$\lim_{\substack{x \rightarrow y \\ x, y \in \partial\Omega}} \frac{(x - y) \cdot \hat{n}(y)}{|x - y|^2} = -\frac{\kappa(y)}{2}, \quad (14)$$

where $\kappa(y)$ is the curvature of $\partial\Omega$ at y . Applying product integration to the G_L term, we get

$$\begin{aligned} \int_{\Gamma} G(y_i, y) \sigma(y) dS(y) &\approx \sum_{\substack{j=1 \\ j \neq i}}^n \left[G(y_i, y_j) \sigma_j s_j \lambda_j^G + G_L(y_i, y_j) \sigma_j \left(w_j^L(x) - s_j \lambda_j^G \right) \right] \\ &\quad + G_0(y_i, y_i) + G_L(y_i, y_i) \sigma_i w_i^L(x) - G_C(y_i, y_i) \frac{\kappa(y_i)}{2}. \end{aligned} \quad (15)$$

2. **Singular, without self-interaction.** If $x \in \partial\Omega$ is either on the source panel Γ , or on a neighboring panel, then the G_C term is still smooth, but we do not have to take the limit at $x \rightarrow y$ into account. This lets us simplify the above to

$$\int_{\Gamma} G(x, y) \sigma(y) dS(y) \approx \sum_{j=1}^n \left[G(x, y_j) \sigma_j s_j \lambda_j^G + G_L(x, y_j) \sigma_j \left(w_j^L(x) - s_j \lambda_j^G \right) \right]. \quad (16)$$

3. **Nearly singular case.** If x is close to Γ , but not on a neighboring panel, then we need to deal with both the singularities in (5). This case occurs when either $x \in \Omega$ is close to $\partial\Omega$, or when $x \in \partial\Omega$ is on a section of the boundary that is distant in arc length or disjoint. The layer potential is then evaluated as

$$\begin{aligned} \int_{\Gamma} G(x, y) \sigma(y) \, dS(y) \approx \sum_{j=1}^n & \left[G(x, y_j) \sigma_j s_j \lambda_j^G \right. \\ & + G_L(x, y_j) \sigma_j \left(w_j^L(x) - s_j \lambda_j^G \right) \\ & \left. + G_C(x, y_j) \sigma_j \left(w_j^C(x) - s_j \lambda_j^G \right) \right]. \end{aligned} \quad (17)$$

Given a target point x , the panels on $\partial\Omega$ are partitioned into two sets: *far* panels, that can be evaluated directly using (11), and *near* panels, that must be evaluated (or corrected), using either (15), (16), or (17).

3 Problem statement

The kernel-split quadrature scheme outlined above is both efficient and accurate when applied to the single and double layer potentials of several PDEs, such as the Laplace, Helmholtz and Stokes equations [9, 7, 13]. However, for the layer potentials of eqs. (1) to (3), the scheme can fail completely. All of these equations have layer potential kernels including second-kind modified Bessel functions, in the forms $K_0(\alpha|x-y|)$ and/or $K_1(\alpha|x-y|)$. As we shall see, this is problematic for the kernel-split quadrature.

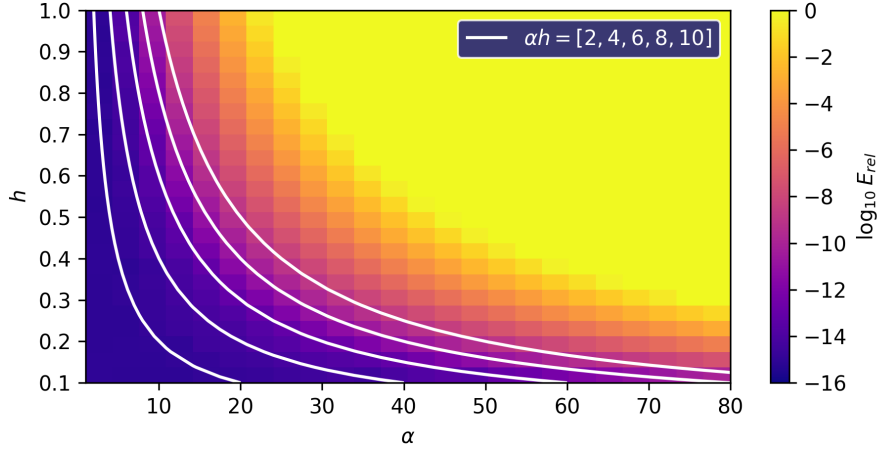


Figure 1: Relative error $E_{rel} = \max_x |u(x) - \tilde{u}(x)|/|u(x)|$, when evaluating the modified Helmholtz single layer potential (23) over a flat panel of length h , using kernel-split quadrature. The maximum is taken over 100 values of x randomly drawn from the box $[-h/2, h/2] \times [0, h/2]$. The white lines are contours of the quantity αh , providing a heuristic motivation for why a criterion of the form (30) is suitable.

As an illustrating example, we study the single layer kernel of the modified Helmholtz equation (1),

$$G(x, y) = K_0(\alpha|x-y|). \quad (18)$$

The split of this kernel is based on using a standard decomposition [12, §10.31] to explicitly write out the singularities in K_0 ,

$$K_0(z) = K_0^S(z) + I_0(z) \log z, \quad (19)$$

where I_0 is a modified Bessel function of the first kind, and K_0^S is the smooth remainder. Inserting this into the kernel (18), after also splitting the logarithm, we identify the terms in (5) as

$$G_0(x, y) = K_0^S(\alpha|x - y|) + I_0(\alpha|x - y|) \log \alpha, \quad (20)$$

$$G_L(x, y) = I_0(\alpha|x - y|), \quad (21)$$

$$G_C(x, y) = 0. \quad (22)$$

Even though $G(x, y)$ goes to zero as $|x - y| \rightarrow \infty$, the functions $G_0(x, y)$ and $G_L(x, y)$ actually grow exponentially as $e^{\alpha|x - y|}$, following the asymptotic $I_0(z) \sim e^z / \sqrt{2\pi z}$ as $z \rightarrow \infty$ [12, §10.30]. As α gets larger, this makes G_L an increasingly bad candidate for polynomial interpolation, which is essential for product integration to be accurate. To illustrate this, we consider the single layer potential with unit density, evaluated using kernel-split quadrature from a flat panel of length h ,

$$u(x) = \int_{-h/2}^{h/2} K_0(x, y) dy, \quad x \notin [-h/2, h/2]. \quad (23)$$

To evaluate this using the kernel-split correction (17), we first write

$$u(x) \approx \sum_{j=1}^n (G(x, y_j) - G_L(x, y_j)) \lambda_j + \int_{-h/2}^{h/2} I_0(\alpha|x - y|) \log |x - y| dy. \quad (24)$$

The remaining integral is evaluated by writing the integrand as a polynomial plus remainder,

$$I_0(\alpha|x - y|) = \sum_{k=1}^n c_k(x) y^{k-1} + r(x, y), \quad (25)$$

and then computing that using product quadrature,

$$\int_{-h/2}^{h/2} I_0(\alpha|x - y|) \log |x - y| dy = \sum_{k=1}^n c_k(x) p_k(x) + \int_{-h/2}^{h/2} r(x, y) \log |x - y| dy, \quad (26)$$

where

$$p_k(x) = \int_{-h/2}^{h/2} y^{k-1} \log |x - y| dy, \quad (27)$$

are integrals that can be computed recursively, starting from exact formulas. The error in the kernel-split quadrature is dominated by the integral in the right-hand side of (24), which integrates the remainder of the polynomial interpolation. To help quantify this remainder, we consider the case $x = 0$. From the power series expansion of I_0 , available at [12, §10.25], we then have that

$$I_0(\alpha|y|) = \sum_{k=0}^{\infty} \frac{\left(\frac{\alpha y}{2}\right)^{2k}}{(k!)^2}, \quad (28)$$

such that, on the interval $y \in [-h/2, h/2]$, the remainder is bounded by

$$r(0, y) \leq \sum_{k=n/2}^{\infty} \frac{\left(\frac{\alpha h}{4}\right)^{2k}}{(k!)^2}. \quad (29)$$

This clearly grows monotonically with the quantity αh . Numerical results indicate that this is the case also for general values of x near Γ , see fig. 1. To ensure that the kernel-split quadrature error remains below some tolerance ϵ , we therefore suggest that α and h must satisfy a criterion on the form

$$\alpha h \leq C_\epsilon, \quad (30)$$

for some constant C_ϵ , which can be determined using numerical experiments. Once determined, we find that this criterion holds well also for general geometries.

The above criterion can also be reformulated as follows: In order to achieve a tolerance ϵ , panel lengths must satisfy

$$h \leq h_{\max} := C_\epsilon / \alpha. \quad (31)$$

The obvious way of achieving this, for a given α , is to discretize $\partial\Omega$ using sufficiently short panels. However, this can result in a discretization with orders of magnitude more points than necessary to resolve the geometry and the layer density.

4 Quadrature by recursive subdivision

To circumvent the problem described above, we here introduce an algorithm for local refinement, based on panel subdivision. Given a single source panel Γ , we assume that it is sufficiently short, relative to the quadrature order n , for both the geometry and the layer density to be well-represented by a polynomial, interpolated at the n quadrature points. We say that it is *well-resolved*. For a given target point x , we can then subdivide Γ into a set of M subpanels $\{\Gamma_i\}_{i=1}^M$, interpolate our known quantities from the quadrature nodes on Γ to the quadrature nodes on those subpanels, and then evaluate the layer potential at x using the subpanels. To ensure accuracy, this subdivision is formed in a way that guarantees that all subpanels either are short enough to satisfy (30), or are sufficiently far away from x , relative to their own length, to not need kernel-split quadrature.

Before we can state our algorithm, a number of preliminaries are needed:

Preimage of target Let $\gamma(t) : \mathbb{R} \rightarrow \mathbb{C}$ be the mapping from the standard interval $[-1, 1]$ to the panel Γ . Then z , such that $\gamma(z) = x$, is the *preimage* of the target point x . The preimage z is real-valued if $x \in \partial\Omega$, and complex-valued otherwise. We here assume that we know the value of z , but $\gamma(t)$ need not be a known function; see [2] for a discussion on how construct a numerical representation.

Subpanels and subintervals A subdivision of Γ is defined by a set of edges in the parametrization, $\{-1 = t_1, t_2, \dots, t_{M+1} = 1\}$, such that a subpanel Γ_i is given by the mapping of the subinterval $[t_i, t_{i+1}]$ under γ . We can, by a linear scaling, define the *local mapping* that maps the standard interval $[-1, 1]$ to Γ_i as

$$\gamma_i(t) = \gamma\left(t_i + \frac{\Delta t_i}{2}(t+1)\right), \quad (32)$$

where $\Delta t_i = t_{i+1} - t_i$. Given the preimage z , the *local preimage* z_i , such that $\gamma_i(z_i) = x$, is given by

$$z_i = \frac{2}{\Delta t_i}(z - t_i) - 1. \quad (33)$$

Near evaluation criterion Given the preimage z of a point x close to a panel (or subpanel) Γ , it is possible to compute an accurate estimate of the quadrature error when evaluating the layer potential using n -point Gauss-Legendre quadrature. Detailed discussions can be found in [1, 2]. To leading order, the error is proportional $\rho(z)^{-2n}$, where ρ is the elliptical radius of the Bernstein ellipse on which z lies,

$$\rho(z) = \left| z + \sqrt{z^2 - 1} \right|, \quad (34)$$

where $\sqrt{z^2 - 1}$ is defined as $\sqrt{z+1}\sqrt{z-1}$ with $-\pi < \arg(z \pm 1) \leq \pi$. For a given kernel G and error tolerance ϵ , it is then possible to introduce cutoff radius R_ϵ , such that kernel-split quadrature must be used for

$$\rho(z) < R_\epsilon, \quad (35)$$

and Gauss-Legendre quadrature is sufficiently accurate otherwise. Later we will use that the inverse of ρ has a particularly simple form in the special case when z lies on the imaginary axis,

$$\begin{aligned} z &= \pm ib, \quad b > 0, \\ \rho(z) &= b + \sqrt{b^2 + 1}, \\ z(\rho) &= \pm i(\rho^2 - 1)/2\rho. \end{aligned} \quad (36)$$

Interpolation and upsampling To interpolate data from the n original Gauss-Legendre nodes on $[-1, 1]$, to m new Gauss-Legendre nodes on a subinterval $[t_i, t_{i+1}] \subset [-1, 1]$, we use barycentric Lagrange interpolation [3]. By *upsampling* we refer to the special case of interpolating from n to $2n$ Gauss-Legendre nodes, both on $[-1, 1]$.

Subinterval length criterion When a new subpanel Γ_i is formed on Γ , we need to check if it satisfies the kernel-split accuracy criterion (30), which requires knowledge of the arc length of the subpanel, denoted h_i . Assuming that $\gamma'(t)$ does not vary rapidly on Γ , a good approximation to h_i is $h_i \approx h\Delta t_i/2$, where h is the arc length of Γ . We can now combine this approximation with (30), to get an accuracy criterion formulated in subinterval size,

$$\Delta t_i \leq \frac{2C_\epsilon}{\alpha h}. \quad (37)$$

In particular, this allows us to write down the maximum length of subintervals on which product integration can be used,

$$\Delta t_{\max} = \frac{2C_\epsilon}{\alpha h}. \quad (38)$$

4.1 Algorithm

Our algorithm proceeds with creating a division of $[-1, 1]$ into subintervals, which corresponds to a division of Γ into subpanels.

For a target point x with preimage z such that $\operatorname{Re} z \in (-1, 1)$, the first step is to create a subinterval centered on $\operatorname{Re} z$, with length set to satisfy both of the conditions (35) and (38). The centering ensures that the subpanels will not introduce new edges or quadrature nodes that are close enough to z to degrade precision. If this initial subinterval has length Δt_c , then the preimage of x in that local frame will be $z_c = ib_c$, with $b_c = 2 \operatorname{Im} z / \Delta t_c$ and (36) is applicable.

If we wish the local preimage z_c to be just beyond the limit where kernel-split quadrature is needed, then we must set Δt_c such that $\rho(z_c) = R_\epsilon$. From (36), we can derive that this is satisfied when $\Delta t_c = \Delta t_{\text{direct}}$,

$$\Delta t_{\text{direct}} = |\operatorname{Im} z| \frac{4R_\epsilon}{R_\epsilon^2 - 1}. \quad (39)$$

For the subinterval to be contained within $[-1, 1]$, it may not be bigger than twice the distance between $\operatorname{Re} z$ and the closest interval edge,

$$\Delta t_{\text{edge}} = 2(1 - |\operatorname{Re} z|) \quad (40)$$

Now we set the initial subpanel as large as possible, while still ensuring that the quadrature from it is accurate, and that it falls within $[-1, 1]$,

$$\Delta t_c = \min(\Delta t_{\text{edge}}, \max(\Delta t_{\text{direct}}, \Delta t_{\text{max}})). \quad (41)$$

This gives us the initial subdivision $\{-1, \operatorname{Re} z - \Delta t_c/2, \operatorname{Re} z + \Delta t_c/2, 1\}$. The center subinterval is now acceptable, and we proceed by recursively bisecting each remaining subinterval until either its length satisfies (37), or the local preimage of x satisfies (35).

For target points such that $\operatorname{Re} z \notin (-1, 1)$, we can skip the process of carefully selecting the length of the nearest subinterval, and proceed immediately with recursive bisection of $\{-1, 1\}$. This completes the algorithm, which we list in its entirety in algorithm 1.

5 Numerical results

To test the robustness of our method across a range of α values, we setup the following test problem: We solve the modified Helmholtz equation (1) inside the annulus defined by a circle of radius 0.3, and a circle of radius 0.6, with Dirichlet boundary conditions given by a fundamental solution (18) located in the inner annulus,

$$(\Delta u - \alpha^2) = 0, \quad x \in \Omega, \quad (42)$$

$$u = K_0(\alpha|x - x_0|), \quad x \in \partial\Omega, \quad (43)$$

$$x_0 = (0.1, 0.1)^T. \quad (44)$$

The exact solution to this problem is equal to the expression for the Dirichlet boundary condition, evaluated in Ω . To solve this problem numerically, we represent the solution using the double layer potential

$$u(x) = \int_{\partial\Omega} \sigma(y) G(x, y) \, dS(y), \quad (45)$$

where G is the double layer kernel,

$$G(x, y) = -\frac{\alpha}{\pi} K_1(\alpha|y - x|) \frac{(y - x) \cdot \hat{n}(y)}{|y - x|}. \quad (46)$$

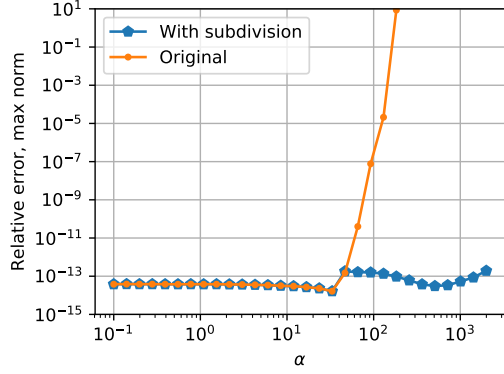
Algorithm 1 Given a panel of length h and a nearby target point with preimage z , create a subdivision of $[-1, 1]$ that allows the the layer potential to be accurately evaluated, using either direct Gauss-Legendre quadrature or kernel-split quadrature.

```

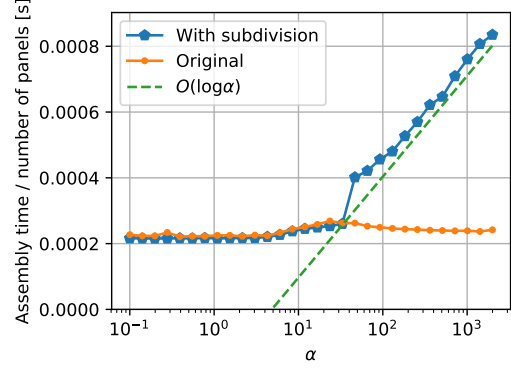
function CREATE_SUBDIVISION( $z, h, \alpha, C_\epsilon, R_\epsilon$ )
  if  $|\operatorname{Re} z| \geq 1$  then                                 $\triangleright$  Preimage outside interval, recursively bisect all of it.
    return RECURSIVE_BISECTION( $-1, 1, R_\epsilon, \Delta t_{\max}, z$ ).
  else
     $\Delta t_{\max} \leftarrow 2C_\epsilon/\alpha h$ 
     $\Delta t_{\text{direct}} \leftarrow 4|\operatorname{Im} z|R_\epsilon/(R_\epsilon^2 - 1)$ 
     $\Delta t_{\text{edge}} = 2(1 - |\operatorname{Re} z|)$ 
     $\Delta t_c \leftarrow \min(\Delta t_{\text{edge}}, \max(\Delta t_{\text{direct}}, \Delta t_{\max}))$ 
     $t_a \leftarrow \operatorname{Re} z - \Delta t_c/2$ 
     $t_b \leftarrow \operatorname{Re} z + \Delta t_c/2$ 
     $\triangleright$  Center interval is now acceptable, recursively bisect remainder subintervals.
     $S_1 \leftarrow \text{RECURSIVE\_BISECTION}(-1, t_a, R_\epsilon, \Delta t_{\max}, z)$ 
     $S_2 \leftarrow \{t_a, t_b\}$ 
     $S_3 \leftarrow \text{RECURSIVE\_BISECTION}(t_b, 1, R_\epsilon, \Delta t_{\max}, z)$ 
    return  $S_1 \cup S_2 \cup S_3$ 
  end if
end function

function RECURSIVE_BISECTION( $t_1, t_2, R_\epsilon, \Delta t_{\max}, z$ )
  if  $t_1 < t_2$  then
     $\Delta t_{\text{sub}} \leftarrow t_2 - t_1$ 
     $z_{\text{sub}} \leftarrow 2(z - t_1)/\Delta t_{\text{sub}} - 1$                                  $\triangleright$  From (33).
    if  $\rho(z_{\text{sub}}) < R_\epsilon$  and  $\Delta t_{\text{sub}} > \Delta t_{\max}$  then                                 $\triangleright$  Using (34).
       $\triangleright$  Kernel-split must be used, but interval still too large. Continue bisection.
       $t_{\text{mid}} \leftarrow t_1 + \Delta t_{\text{sub}}/2$ 
       $S_1 \leftarrow \text{RECURSIVE\_BISECTION}(t_1, t_{\text{mid}}, R_\epsilon, \Delta t_{\max}, z)$ 
       $S_2 \leftarrow \text{RECURSIVE\_BISECTION}(t_{\text{mid}}, t_2, R_\epsilon, \Delta t_{\max}, z)$ 
      return  $S_1 \cup S_2$ 
    end if
  end if
  return  $\{t_1, t_2\}$                                  $\triangleright$  Subinterval passed.
end function

```



(a) Error when evaluating the layer potential close to the boundary, relative error in max norm computed as $\|u - u_{\text{ref}}\|_{\infty} / \|\sigma\|_{\infty}$.



(b) Time to assemble the matrix blocks that correspond to neighboring panels, which is where the log-correction need to be added.

Figure 2: Comparison of the original kernel-split algorithm, denoted “Original”, and our adaptive algorithm, denoted “With subdivision”, when solving our test problem for a large range of α . We test the solution up to $\alpha \approx 2000$; for larger values of α the solution is identically zero in the entire domain.

Enforcing the boundary condition gives us a second kind integral equation in σ ,

$$\sigma(x) + \int_{\partial\Omega} \sigma(y) G(x, y) \, dS(y) = K_0(\alpha|x - x_0|), \quad x \in \partial\Omega. \quad (47)$$

We solve this using the Nyström method, discretizing the boundary using 16-point Gauss-Legendre panels, with 15 panels on the inner circle, and 30 panels on the outer. For the bounds (37) and (39) we use $C_\epsilon = 4$ and $R_\epsilon = 3$ (empirically determined). Following the notation of (5), the kernel-split of (46) is given by

$$G_L(x, y) = -\frac{\alpha}{\pi} I_1(\alpha|y - x|) \frac{(y - x) \cdot \hat{n}(y)}{|y - x|}, \quad (48)$$

$$G_C(x, y) = -\frac{1}{\pi}. \quad (49)$$

For a large range of α values, we solve the integral equation, and then evaluate the solution at 15 random points on a circle of radius 0.301 (very close to the inner boundary). The results, shown in fig. 2 demonstrate that our subdivision algorithm is capable of avoiding the catastrophic loss of accuracy otherwise present above a threshold α , and that the additional cost incurred from it is proportional to $\log \alpha$. Around one digit of accuracy appears to be lost after the adaptive quadrature is activated, presumably due to the additional interpolation steps involved.

The present test problem is somewhat difficult to work with, since the solution to the modified Helmholtz equation decays exponentially fast. This limits the largest value of α that we can test, as noted in the caption to fig. 2. To test larger ranges we can solve problems whose solutions do not decay as fast, such as the modified Stokes equations or the modified biharmonic equation. Such tests will be reported at a later date.

6 Conclusions

We present a robust recursive algorithm that allows the method of Helsing et al. to be applied, for any α , to the modified Helmholtz equation, modified biharmonic equation and modified Stokes equations. Before, this was not possible for large α , which corresponds to small timesteps with semi-implicit marching schemes for the heat equation and the time-dependent Stokes and Navier-Stokes equations. Our algorithm is fully adaptive, and the additional computational time it requires scales as $\log \alpha$. Our choice of the parameters C_ϵ and R_ϵ is based on numerical observations and provide excellent results. We will at a later date expand this report by adding an error analysis, together with error estimates that can be used for parameter selection.

Acknowledgments

The authors gratefully acknowledge the support from the Knut and Alice Wallenberg Foundation under grant no. 2016.0410 (L.a.K.), and by the Swedish Research Council under Grant No. 2015-04998 (F.F. and A.K.T.)

References

- [1] L. af Klinteberg and A.-K. Tornberg. Error estimation for quadrature by expansion in layer potential evaluation. *Adv. Comput. Math.*, 43(1):195–234, 2017. doi:10.1007/s10444-016-9484-x.
- [2] L. af Klinteberg and A.-K. Tornberg. Adaptive quadrature by expansion for layer potential evaluation in two dimensions. *SIAM J. Sci. Comput.*, 40(3):A1225–A1249, 2018. doi:10.1137/17M1121615.
- [3] J.-P. Berrut and L. N. Trefethen. Barycentric Lagrange interpolation. *SIAM Rev.*, 46(3):501–517, 2004. doi:10.1137/S0036144502417715.
- [4] M. Catherine A. Kropinski and B. Quaife. Fast integral equation methods for Rothe’s method applied to the isotropic heat equation. *Comput. Math. with Appl.*, 61:2436–2446, 2011. doi:10.1016/j.camwa.2011.02.024.
- [5] C. S. Chen, X. Jiang, W. Chen, and G. Yao. Fast solution for solving the modified Helmholtz equation with the method of fundamental solutions. *Commun. Comput. Phys.*, 17(3):867–886, 2015. doi:10.4208/cicp.181113.241014a.
- [6] L. Greengard and M. C. Kropinski. An integral equation approach to the incompressible Navier–Stokes equations in two dimensions. *SIAM J. Sci. Comput.*, 20(1):318–336, 1998. doi:10.1137/S1064827597317648.
- [7] J. Helsing and A. Holst. Variants of an explicit kernel-split panel-based Nyström discretization scheme for Helmholtz boundary value problems. *Adv. Comput. Math.*, 41(3):691–708, 2015. doi:10.1007/s10444-014-9383-y.
- [8] J. Helsing and S. Jiang. On integral equation methods for the first Dirichlet problem of the biharmonic and modified biharmonic equations in nonsmooth domains. *SIAM J. Sci. Comput.*, 40(4):A2609–A2630, 2018. doi:10.1137/17M1162238.

- [9] J. Helsing and R. Ojala. On the evaluation of layer potentials close to their sources. *J. Comput. Phys.*, 227(5):2899–2921, 2008. doi:10.1016/j.jcp.2007.11.024.
- [10] S. Jiang, M. C. A. Kropinski, and B. D. Quaife. Second kind integral equation formulation for the modified biharmonic equation and its applications. *J. Comput. Phys.*, 249:113–126, 2013. doi:10.1016/j.jcp.2013.04.034.
- [11] M. C. A. Kropinski and B. D. Quaife. Fast integral equation methods for the modified Helmholtz equation. *J. Comput. Phys.*, 230(2):425–434, 2011. doi:10.1016/j.jcp.2010.09.030.
- [12] NIST. Digital library of mathematical functions. Release 1.0.16 of 2017-09-18. URL <http://dlmf.nist.gov/>.
- [13] R. Ojala and A.-K. Tornberg. An accurate integral equation method for simulating multi-phase Stokes flow. *J. Comput. Phys.*, 298:145–160, 2015. doi:10.1016/j.jcp.2015.06.002.
- [14] Y. N. Vorobjev. Modeling of electrostatic effects in macromolecules. In L. A., editor, *Comput. Methods to Study Struct. Dyn. Biomol. Biomol. Process. From Bioinforma. to Mol. Quantum Mech.*, pages 163–202. Springer International Publishing, Cham, 2019. ISBN 978-3-319-95843-9. doi:10.1007/978-3-319-95843-9_6.
- [15] H.-X. Zhou and X. Pang. Electrostatic interactions in protein structure, folding, binding, and condensation. *Chem. Rev.*, 118(4):1691–1741, 2018. doi:10.1021/acs.chemrev.7b00305.